Observations of the Kondo effect and its coexistence with ferromagnetism in a magnetically undoped metal oxide nanostructure

Keshab R. Sapkota, F. Scott Maloney, and Wenyong Wang*
Department of Physics and Astronomy, University of Wyoming, Laramie, Wyoming 82071, USA

(Received 4 July 2017; revised manuscript received 30 March 2018; published 30 April 2018)

In this work, we report unusual observations of Kondo effect and coexistence of Kondo effect and ferromagnetism in indium tin oxide (ITO) nanowires that were synthesized without incorporating any magnetic impurities. The temperature-dependent resistivity (ρ-T) data exhibited an upturn below 80 K and then tended to saturate below 10 K. The ρ-T and magnetoresistance data were analyzed using the n-channel Kondo model, and from the obtained values of $S = 1$ and $n \sim 1$, the nanowires were expected to be an underscreened Kondo system. A model was also proposed to explain the formation of localized $S = 1$ spin centers in the ITO nanowires. This work could provide insights into the understanding of spin-related novel phenomena in metal oxide nanostructures.

DOI: 10.1103/PhysRevB.97.144425

It is well known that the Kondo effect arises when spin-flip scatterings of conduction electrons by localized spins cause anomalous upturn of material resistivity below a certain temperature [1,2]. Since the first discovery of the Kondo effect in 1930 in normal metals that contain small amounts of magnetic impurities, this effect has been observed in different materials including dilute magnetic alloys, semiconductor quantum dots, carbon nanotubes, and graphene [1,3–6]. Kondo system can exhibit interesting magnetic behaviors depending on the spin-flip scattering process. For example, in an n-channel Kondo system, the localized spin $\boldsymbol{S}$ interacts with conduction electrons through n different orbital channels, and ferromagnetism (FM) can be established if the interaction between the conduction electrons and local spins leaves underscreened localized spins with a new spin magnitude $\boldsymbol{S}'$ such that $0 < \boldsymbol{S}' < \boldsymbol{S}$ [7]. However, thus far there are only few materials that have been reported to exhibit the coexistence of underscreened Kondo scattering and FM, and none of them are magnetically undoped metal oxide nanostructures [8–10].

Indium tin oxide (ITO) is a highly conductive, wide-band-gap semiconductor in which electrons are majority charge carriers. It is a widely used transparent electrode and can be found in flat panel displays, optical coatings, and solar cells [11]. In addition to its use as thin films, ITO can be easily grown into nanostructures, which makes it a good candidate material for nanoscale device applications [12]. In this work we synthesized ITO nanowires without incorporating any magnetic impurities and characterized their electrical and magnetic properties. Unexpectedly, we observed Kondo effect in these ITO nanowires that did not contain any d- or f-orbital unpaired spins. There have been reports on Kondo effect observed in metal oxides, but these metal oxides usually contain d- or f-orbital unpaired spins from the doping of d- or f-block elements [13–15]. The d- or f-block elements are not necessarily magnetic, but when they possess unpaired d- or f-orbital spins that lie deep in the energy band and are localized states, such doping can lead to the Kondo effect. However, Kondo scattering in metal oxides in the absence of d- or f-orbital spin impurities is a rarely observed phenomenon in condensed-matter physics [16], and in this paper we report such an unusual observation. In addition, we further conducted magnetization measurement and observed ferromagnetic behavior of the ITO nanowires. Ferromagnetic behavior of ITO nanostructures has been reported before [17–19]; however, the coexistence of Kondo effect and ferromagnetism in ITO or other types of metal oxides that do not contain magnetic impurities is again a seldom-reported phenomenon. We analyzed the experimental data using the n-channel Kondo model, and found that the ferromagnetic behavior of ITO nanowires could be attributed to the underscreened local spins. We also proposed a model to explain the formation of local spins of magnitude 1 in the ITO nanowires.

The ITO nanowires were synthesized using a vapor-liquid-solid growth process, and nanowire four-probe testbeds were fabricated via standard e-beam lithography process (Supplemental Material [20]) [21–24]. Figure 1 shows the temperature-dependent resistivity (ρ-T) measurement data of an ITO nanowire without and with the application of an external magnetic field, and Fig. 1 inset shows a SEM image of the four-probe nanowire test structure. The resistivity of ITO can depend on Sn concentration, oxygen vacancy, defect state, surface treatment, and other factors [12,24,25]. The measured electrical resistivity of the ITO nanowires at 300 K was $\sim 404\,\mu\Omega \cdot \mathrm{cm}$, which was within the range of previously reported values of ITO nanowires or thin films [24,25]. The temperature-dependent resistivity of the ITO nanowire was measured between 300 and 5 K. As shown in Fig. 1, when the temperature was initially decreased, the resistivity of the ITO nanowire also decreased and the derivative $d\rho/dT > 0$, exhibiting a metallic ρ-T behavior. However, when the temperature was further decreased the ITO nanowire resistivity started to increase, with a resistivity minimum occurring at $T_{\mathrm{min}} \sim 80\,\mathrm{K}$, and when the temperature reached below 10 K the resistivity tended to saturate. As can be seen in Fig. 1, the application of an external magnetic field during ρ-T

*wwang5@uwyo.edu

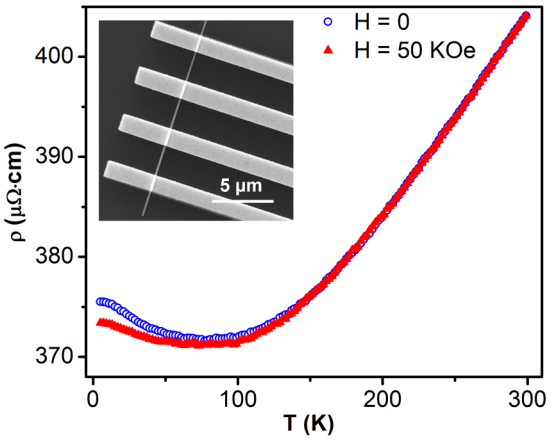

FIG. 1. Temperature-dependent resistivity measurement of an ITO nanowire without and with the application of magnetic field. The inset is the SEM image of a single nanowire device.

measurement lowered the ITO nanowire resistivity at temperatures below 140 K, while the resistivity minimum still occurred at ∼80 K. The observed metallic behavior of the ITO nanowire resistivity could be explained by the Bloch-Gruneisen model, in which the temperature-dependent resistivity is the result of the interaction between conduction electrons and acoustic phonons [26]:

$$\rho_{BG}(T) = \rho_0 + \rho_{e-ph}(T) = \rho_0 + \alpha\left(\frac{T}{\theta_D}\right)^5 \int_0^{\theta_D/T} \frac{x^5}{(e^x-1)(1-e^x)}dx, \quad (1)$$

where ρ_0 is the residual resistivity, α is a constant that depends on electron-phonon coupling, Debye frequency, and plasma frequency, and θ_D is the Debye temperature. This equation fitted the ρ-T data between 300 and 140 K ($d\rho/dT > 0$ region) well, as shown in Fig. 2 inset, from which $\rho_0 = 370.2\ \mu\Omega \cdot$ cm, $\alpha = 665\ \mu\Omega \cdot$ cm, and $\theta_D = 912$ K were obtained, and these numbers were in agreement with previously reported values [25]. The neutral defects and ionized impurity centers such as doubly charged O vacancies and singly charged Sn sites in the ITO nanowires were responsible for this observed high residual resistivity, which produced strong scatterings of the conduction electrons in the material [24,27].

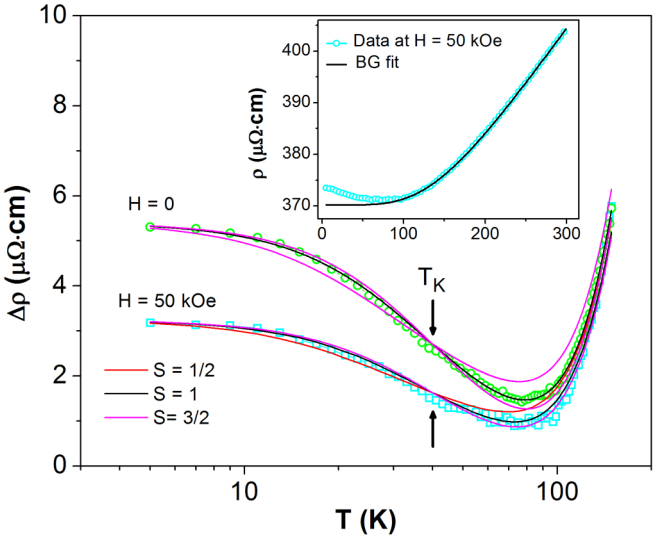

FIG. 2. Fitting of the temperature-dependent resistivity data at low temperature with the NRG n-channel Kondo model. The inset shows the Bloch-Gruneisen fit of the ρ-T data at high temperature.

Using free-electron approximation, the Fermi wavelength λ_F and the electron mean-free path at room temperature $l_{300\,\mathrm{K}}$ in the ITO nanowires were estimated to be roughly 1.9 and 2.9 nm, respectively, indicating the ITO nanowires in this study were a 3D system [27,28]. In addition, the product of k_F and $l_{300\,\mathrm{K}}$ yielded a value of ∼9.5. It is well known that if the $k_F l$ value of a system is much larger than 1, then this system qualifies as a weakly perturbed system according to the scaling theory of localization [29]. As Fig. 1 shows, the ITO nanowire resistivity at low temperature was affected by external magnetic field, suggesting the resistivity minimum behavior could be associated with spin-dependent scatterings. Various mechanisms such as weak localization, electron-electron scattering, or Kondo-related scattering could cause this resistivity minimum behavior. Among them, the weak localization effect is common in disordered materials. Disorders exist in materials in the forms of impurities, defects, and interstitials, and the random disorder potentials can interact with free electrons and give rise to the localization effect. If the effect of disorders is perturbative on conduction electrons, as commonly observed in systems with $k_F l \gg 1$, the localization effect is weak and the temperature-dependent resistivity scales approximately as $\rho_{wl}(T) \sim \rho_0 - {\rho_0}^2 A_1 T^{3/2}$ in three dimensions, where A_1 is a constant [29]. It could be possible that the combined effects of weak localization and electron-phonon scattering described by Eq. (1) produced the resistivity minimum. At low temperature, electron-electron (e-e) interaction could also become a dominant factor that affects the resistivity. The temperature-dependent resistivity correction due to e-e interaction can take the form of $\rho_{e-e}(T) \sim \rho_0 - {\rho_0}^2 A_2 T^{1/2}$, where A_2 is a constant [29–31]. The electron-electron interaction combined with electron-phonon interaction could produce an upturn in the resistivity at low temperature; however, it is insensitive to external magnetic field and thus cannot be applied to our situation [31,32]. Since the weak localization effect is magnetic-field-dependent, we analyzed the ITO low-temperature ρ-T data using two models considering (a) combined effects of $\rho_{wl}(T)$ and $\rho_{e-ph}(T)$ and (b) combined effects of $\rho_{wl}(T)$, $\rho_{e-e}(T)$, and $\rho_{e-ph}(T)$, respectively. The least-squares fitting results are presented in Supplemental Material, section 4 [20], which showed that neither model could fit the experimental data.

The observed ITO nanowire resistivity minimum and saturation behavior at low temperature could be explained by taking into account the n-channel Kondo scattering mechanism. Although the ITO nanowires exhibited a relatively high resistivity, as previous reports have shown, it is not uncommon to observe Kondo effect in high-resistivity systems [10,33]. In an n-channel Kondo system, an embedded local spin $\boldsymbol{S}$ interacts with conduction electrons through n different orbital channels, and the scattering mechanism depends mainly on three parameters: the local spin $\boldsymbol{S}$, the number of channels n, and the Kondo temperature T_K [34]. If the major

contributions to the ITO nanowire resistivity were from phonon scattering and local spin scattering, then it could be expressed as $\rho(T) = \rho_0 + \rho_{e-ph}(T) + \rho_s(T)$, where $\rho_{e-ph}(T)$ is from phonon scattering described by Eq. (1) and $\rho_s(T)$ is related to local spin scattering. Possible mechanisms associated with the formation of local spin $\boldsymbol{S}$ in ITO nanowires without any magnetic impurities will be discussed next in this paper. Using the approach of numerical renormalization group (NRG) calculation, $\rho_s(T)$ for an n-channel Kondo system can be expressed as [35,36]

$$\rho_s(T) = \rho_s(0)\left[1 + (2^{1/S} - 1)\left(\frac{T}{T_K}\right)^2\right]^{-S}, \qquad (2)$$

and for a given spin $\boldsymbol{S}$, the Kondo temperature T_K is defined as $\rho_s(T_K) = \frac{1}{2}\rho_s(0)$. It is worth mentioning that the resistivity saturation at low temperature, as observed in the ITO nanowires, is a signature behavior of $\rho_s(T)$ obtained by NRG calculation. Following previously published procedures [35], the residual resistivity ρ_0 of 370.2 $\mu\Omega \cdot$ cm was subtracted from the ρ-T data and the subsequent experimental data set between 5 and 140 K was fitted using the NRG Kondo model $\Delta\rho(T) = \rho(T) - \rho_0 = \rho_{e-ph}(T) + \rho_s(T)$. The fitting was performed for $\boldsymbol{S} = 1/2$, 1, and 3/2, without and with the magnetic field. As Fig. 2 shows, the best fit was obtained with $\boldsymbol{S} = 1$ in either case and T_K was estimated to be 39.8 K. The obtained T_K did not match T_{min}; however, such a mismatch has been frequently observed in NRG Kondo systems [35,37].

To further investigate the n-channel Kondo scattering phenomenon, the magnetoresistance (MR) of the ITO nanowires was characterized at 5 K in the magnetic field range of ±10 kOe, which was applied perpendicular to the nanowire length axis. Negative MR with a magnitude of less than 1% was observed and is shown in Fig. 3(a). Similar MR behavior was also observed when the magnetic field was applied parallel to the nanowire length axis as shown in Fig. 3(a) inset. Magnetization measurement of the ITO nanowires as a function of applied magnetic field was also performed at 10 K and the result is presented in Fig. 3(b), where the magnetization curve clearly exhibited ferromagnetic behavior, which was in agreement with previous reports [17–19]. Since the magnetization signal from a single nanowire was too weak to be measurable, the magnetization measurement was conducted on a film of ITO nanowires. The two MR curves shown in Fig. 3(a) inset were isotropic, suggesting this MR was less likely to be associated with the ferromagnetic behavior that usually produces anisotropic MR because of the easy and hard axes of the magnetization vector [38]. One possible mechanism for isotropic MR with small magnitude could be the weak localization effect, which often produces negative MR due to the suppression of this effect under an external magnetic field [39]. We conducted MR data fitting using the weak localization model, and the result is presented in Supplemental Material, section 5 [20]. As can be seen from this analysis, the observed ITO nanowire negative MR could not be associated with the weak localization correction to the resistivity. This lack of substantial weak localization contribution in the ferromagnetic ITO nanowires could be related to the suppression of the weak localization by internal magnetic field due to the ferromagnetic exchange interaction and related internal spin dynamics [40,41].

Kondo spin scattering, on the other hand, generally produces isotropic negative MR with small magnitude [42,43]. Therefore, MR data analysis and modeling were carried out by considering the local spin scattering in an n-channel Kondo system. Following the NRG n-channel Kondo model, the magnetoresistivity $\rho_s(H, T)$ associated with the scatterings of electrons with spin $\sigma = \pm 1/2$ in a system with small concentration of Kondo spin $\boldsymbol{S}$ is given by [44]

$$\rho_s^{-1}(H,T) = \frac{n_e\, e^2}{2m^*} \sum_{\sigma} \int_{-\infty}^{+\infty} d\omega\, A_\sigma(\omega, T, H)\left(-\frac{\partial f(\omega)}{\partial \omega}\right), \qquad (3)$$

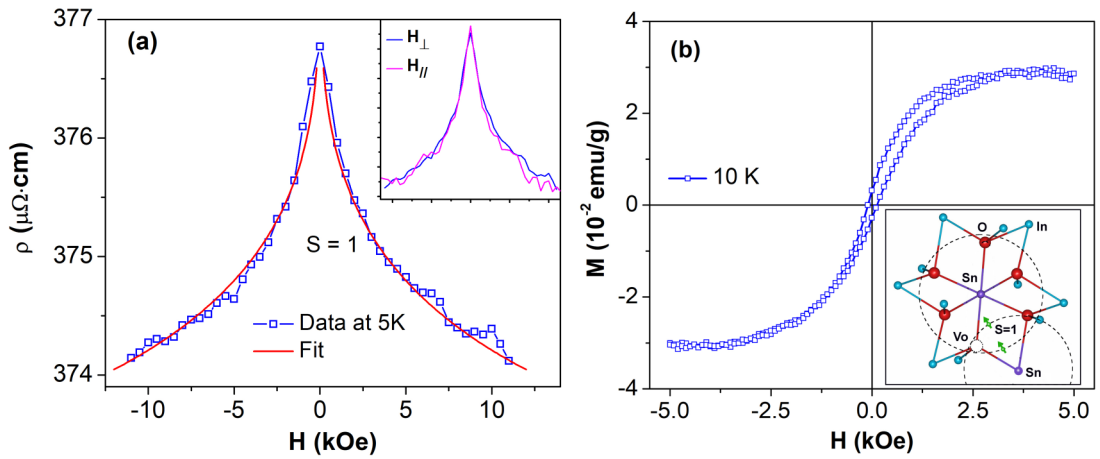

FIG. 3. Transport and magnetization measurements of the ITO nanowires. (a) Magnetoresistance measurement and data fitting using the NRG n-channel Kondo model. Inset shows the MR measurements at parallel and perpendicular magnetic field with respect to the nanowire length axis. (b) Field-dependent magnetization measurement of the ITO nanowires, which shows their ferromagnetic behavior. Inset is the schematic of the formation of a local spin-1 center in an ITO crystal.

where $A_\sigma(\omega, T, H)$ is the spectral density, $f(\omega)$ is the Fermi function, and n_e, m^*, and e are electron concentration, electron mass, and charge, respectively. Considering Fermi-liquid behavior and following the Friedel Sum rule, at $T = 0$ and $\omega = 0$ the spectral density can be expressed as $A_\sigma(\omega = 0, T = 0, H) = \frac{1}{\pi^2 N(0)} \sin^2 \delta_\sigma(H)$ [44,45], where $\delta_\sigma(H)$ is the magnetic-field-dependent phase shift acquired by an electron of spin σ during the scattering by local spin $\boldsymbol{S}$ and $N(0)$ is the unperturbed electron density of states per spin at $\omega = 0$. After substituting $A_\sigma(\omega = 0, T = 0, H)$ into Eq. (3), the following expression was obtained:

$$\rho_s(T=0,H) = \frac{2\, m^* \pi^2 N(0)}{n_e\, e^2} \times \left[\sin^2\delta_{\frac{1}{2}}(H) + \sin^2\delta_{-\frac{1}{2}}(H)\right]^{-1}, \quad (4)$$

where the scattered electron phase shift $\delta_{\pm 1/2}(H)$ is related to local spin magnetization $M_i(H)$ and is given by $\delta_{\pm 1/2}(H) = \frac{\pi}{2}[1 \pm 2M_i(H)]$ [34,44]. For an n-channel Kondo system, $M_i(H)$ depends on the relationship between the channel number n and local spin $\boldsymbol{S}$, where each channel carries ½ spin. There are three possible situations: (1) $n = 2\boldsymbol{S}$; (2) $n < 2\boldsymbol{S}$; and (3) $n > 2\boldsymbol{S}$ [7,34]. For $n = 2\boldsymbol{S}$, the local spin $\boldsymbol{S}$ is completely screened by the spins of the scattering electrons through n channels. The ground state is nondegenerate and each impurity electron forms a singlet state with an electron in each orbital channel. For $n < 2\boldsymbol{S}$, the scattering electrons cannot completely quench the local spin $\boldsymbol{S}$ but instead produce a net spin of $\boldsymbol{S}-n/2$, and the net spins can have exchange interaction among them and give rise to ferromagnetism. For $n > 2\boldsymbol{S}$, the scattering electrons overcompensate the local spin $\boldsymbol{S}$, which causes non-Fermi liquid behavior and can produce antiferromagnetic interaction. The expressions of $M_i(H)$ for $g\mu_B H \ll K_B T$ corresponding to the three aforementioned situations are [7]

$$\begin{aligned} M_i(H) &\sim \frac{g\mu_B H}{2\pi\ K_B T_K} + k_1\left(\frac{g\mu_B H}{K_B T_K}\right)^3 + \ldots \ ; \quad n = 2\boldsymbol{S} \\ M_i(H) &\sim \left(S - \frac{n}{2}\right)\left(1 - \frac{1}{\log(g\mu_B H/K_B T_K)}\right); \quad n < 2\boldsymbol{S} \\ M_i(H) &\sim \left(\frac{g\mu_B H}{K_B T_K}\right)^\beta; \quad n > 2\boldsymbol{S}, \end{aligned} \quad (5)$$

where g is the g factor, μ_B is the Bohr magneton, K_B is the Boltzmann constant, k_1 is a constant, and β is a number depending only on n and $\boldsymbol{S}$. Fittings were carried out for the scenarios of $n = 2\boldsymbol{S}$, $n < 2\boldsymbol{S}$, and $n > 2\boldsymbol{S}$, using $\boldsymbol{S} = 1$ and $T_K = 39.8$ K as obtained from the ρ-T data analysis. The best fit was obtained for $n < 2\boldsymbol{S}$ as shown in Fig. 3(a), and the value of the main fitting parameter n was found to be 1.12. The fitting of the MR data thus suggested that the ITO nanowire was a one-channel Kondo system, and the value of n being slightly higher than 1 could be associated with the presence of a small number of spin-½ centers along with majority spin-1 centers in the ITO nanowires.

The analysis of the ρ-T and MR data above suggested that the ITO nanowires could be a one-channel Kondo system with majority spin $\boldsymbol{S} = 1$ impurity centers, and the underscreened spin centers ($\boldsymbol{S} - n/2 > 0$) could trigger the long-range ferromagnetic exchange interaction via the Ruderman-Kittel-Kasuya-Yosida (RKKY) exchange interaction that was commonly observed in ferromagnetic Kondo lattices where competition between Kondo screening and RKKY interaction existed [13]. Other possible mechanisms such as percolation among bound magnetic polarons created over the underscreened spin centers could also establish the long-range ferromagnetic ordering in the material [46].

It is known that electrons are majority carriers in undoped In_2O_3 due to the presence of oxygen vacancies and each oxygen vacancy contributes two conduction electrons, which can be expressed by the Kroger-Vink notation: $(O^{2-})_O^x \rightarrow \frac{1}{2}O_2(g) + V_O^{**} + 2e'$ [47], where the subscript indicates the site at which a defect is located and the superscript denotes the charge of the defect: ^{x} represents a neutral defect, * represents a positive defect, and $'$ represents a negative defect. For example, $(O^{2-})_O^x$ represents a neutral oxygen ion occupying an oxygen site. When Sn is incorporated into In_2O_3, it typically replaces In^{3+} with Sn^{4+} [48]. Each $(Sn^{4+})^*_{In3+}$ donates one electron and the conductivity of In_2O_3 thus increases linearly with the increase of Sn^{4+} up to a few percent of Sn doping and then it starts to saturate [22,49]. The electron contributions by the vacancies and Sn^{4+} donors in ITO nanowires thus could raise the Fermi level close enough to the conduction band, resulting in metallic conductivity as observed in the ρ-T data (Fig. 1). On the other hand, at or near the surface of an oxide nanowire, the number of available nearest neighbors was reduced and the density of states decreased accordingly, which could produce relatively localized states such that a positive charge center (e.g., vacancy or positive ion) in the vicinity of the surface could trap an electron in a hydrogenic orbital [19]. In the ITO nanowire, the positive charge center $(Sn^{4+})^*_{In3+}$ in the vicinity of the surface along with V_O as a neighboring site could capture one electron in a hydrogenic orbital and form a spin-½ center. However, if two $(Sn^{4+})^*_{In3+}$ sites existed in the neighborhood of a V_O, then each $(Sn^{4+})^*_{In3+}$ site could capture one electron and the two $(Sn^{4+})^*_{In3+}$ sites together with the V_O site could form a $2\{(Sn^{4+})^*_{In3+}e'\}V_O^{**}$ complex as $(O^{2-})_O^x + 2(Sn^{4+})^*_{In3+} \rightarrow \frac{1}{2}O_2(g) + 2\{(Sn^{4+})^*_{In3+}\, e'\}V_O^{**}$. This $2\{(Sn^{4+})^*_{In3+}e'\}V_O^{**}$ complex could produce an $\boldsymbol{S} = 1$ spin center when the two electronic states in the complex interacted to form a spin-triplet state, which is depicted in the schematic shown in Fig. 3(b) inset. Therefore, in ITO nanowires both spin-½ and spin-1 centers could exist, and with nearly 1 Sn atom per 2 In atoms in the ITO crystal (Supplemental Material [20]), conditions for forming the $2\{(Sn^{4+})^*_{In3+}e'\}V_O^{**}$ complex could be easily achieved to realize a majority of spin-1 centers. These local spins were responsible for the observed Kondo scattering as well as the ferromagnetic behavior in the ITO nanowires as discussed previously.

In summary, in this study we observed Kondo effect and coexistence of Kondo effect and ferromagnetism in ITO nanowires that did not contain any magnetic impurities. The obtained ρ-T and MR data were analyzed using the n-channel Kondo model obtained from the NRG theory. The ITO nanowires were found to be a one-channel Kondo system with local spin $\boldsymbol{S} = 1$, and such spin-1 centers could be realized when $2\{(Sn^{4+})^*_{In3+}e'\}V_O^{**}$ complexes were formed due to the

presence of oxygen vacancies in the vicinity of Sn^{4+} sites. In addition, each of the local $S = 1$ spin left $S - n/2 \sim 0.44$ residual spin due to the undercompensated one-channel Kondo scattering, which could trigger long-range ferromagnetic ordering in the ITO nanowires. The ferromagnetism in the ITO nanowires could be reasonably explained using the proposed model; however, since thus far there are only few reports on the observation of coexistence of Kondo effect and ferromagnetism, further studies are needed especially on metal oxide nanowires to fully understand the mechanisms of this interesting phenomenon.

This work was supported by the U.S. Department of Energy, Office of Basic Energy Sciences, Division of Materials Sciences and Engineering under Award No. DE–FG02–10ER46728.

[1] J. Kondo, Prog. Theor. Phys. **32**, 37 (1964).
[2] J. Kondo, Proc. Jpn. Acad. Ser. B **82**, 328 (2006).
[3] S. Kondo, D. C. Johnston, C. A. Swenson, F. Borsa, A. V. Mahajan, L. L. Miller, T. Gu, A. I. Goldman, M. B. Maple, D. A. Gajewski, E. J. Freeman, N. R. Dilley, R. P. Dickey, J. Merrin, K. Kojima, G. M. Luke, Y. J. Uemura, O. Chmaissem, and J. D. Jorgensen, Phys. Rev. Lett. **78**, 3729 (1997).
[4] A. Brinkman, M. Huijben, M. van Zalk, J. Huijben, U. Zeitler, J. C. Maan, W. G. van der Wiel, G. Rijnders, D. H. A. Blank, and H. Hilgenkamp, Nat. Mater. **6**, 493 (2007).
[5] D. Goldhaber-Gordon, J. Göres, M. A. Kastner, H. Shtrikman, D. Mahalu, and U. Meirav, Phys. Rev. Lett. **81**, 5225 (1998).
[6] J. H. H. Chen, W. G. Cullen, E. D. Williams, M. S. Fuhrer, L. Li, W. G. Cullen, E. D. Williams, and M. S. Fuhrer, Nat. Phys. **7**, 535 (2011).
[7] A. M. Tsvelick and P. B. Wiegmann, J. Stat. Phys. **38**, 125 (1985).
[8] S. Berger, A. Galatanu, G. Hilscher, H. Michor, C. Paul, E. Bauer, P. Rogl, M. Gómez-Berisso, P. Pedrazzini, J. G. Sereni, J. P. Kappler, A. Rogalev, S. Matar, F. Weill, B. Chevalier, and J. Etourneau, Phys. Rev. B **64**, 134404 (2001).
[9] K. S. Burch, A. Schafgans, N. P. Butch, T. A. Sayles, M. B. Maple, B. C. Sales, D. Mandrus, and D. N. Basov, Phys. Rev. Lett. **95**, 046401 (2005).
[10] L. Zhu, G. Woltersdorf, and J. Zhao, Sci. Rep. **6**, 1 (2016).
[11] J. Wager, Science **300**, 1245 (2003).
[12] Q. Wan, E. N. Dattoli, W. Y. Fung, W. Guo, Y. Chen, X. Pan, and W. Lu, Nano Lett. **6**, 2909 (2006).
[13] C. Krellner, N. S. Kini, E. M. Brüning, K. Koch, H. Rosner, M. Nicklas, M. Baenitz, and C. Geibel, Phys. Rev. B **76**, 104418 (2007).
[14] Y. Li, R. Deng, W. Lin, Y. Tian, H. Peng, J. Yi, B. Yao, and T. Wu, Phys. Rev. B **87**, 155151 (2013).
[15] T. P. Sarkar, K. Gopinadhan, M. Motapothula, S. Saha, Z. Huang, S. Dhar, A. Patra, W. M. Lu, F. Telesio, I. Pallecchi, Ariando, D. Marré, and T. Venkatesan, Sci. Rep. **5**, 13011 (2015).
[16] J. Y. Yang, Y. L. Han, L. He, R. F. Dou, C. M. Xiong, and J. C. Nie, Appl. Phys. Lett. **100**, 202409 (2012).
[17] B. Xia, Y. Wu, H. W. Ho, C. Ke, W. D. Song, C. H. A. Huan, J. L. Kuo, W. G. Zhu, and L. Wang, Physica B **406**, 3166 (2011).
[18] G. G. Khan, S. Ghosh, G. D. M. Ayan Sarkar, G. Mandal, U. Manju, N. Banu, and B. N. Dev, J. Appl. Phys. **118**, 074303 (2015).
[19] G. S. Chang, J. Forrest, E. Z. Kurmaev, A. N. Morozovska, M. D. Glinchuk, J. A. McLeod, A. Moewes, T. P. Surkova, and N. H. Hong, Phys. Rev. B **85**, 165319 (2012).
[20] See Supplemental Material at http://link.aps.org/supplemental/10.1103/PhysRevB.97.144425 for the synthesis and characterization of nanowires and analysis of transport data using electron-electron interactions and weak localization theories.
[21] K. R. Sapkota, W. Chen, F. S. Maloney, U. Poudyal, and W. Wang, Sci. Rep. **6**, 35036 (2016).
[22] G. B. Gonzalez, J. B. Cohen, J. H. Hwang, T. O. Mason, J. P. Hodges, and J. D. Jorgensen, J. Appl. Phys. **89**, 2550 (2001).
[23] N. Nadaud, N. Lequeux, M. Nanot, J. Jovenstitut, and T. Roisnel, J. Solid State Chem. **135**, 140 (1998).
[24] R. T. H. Bel, T. Ban, Y. Ohya, and Y. Takahashi, J. Appl. Phys. **83**, 2631 (1998).
[25] S. P. Chiu, H. F. Chung, Y. H. Lin, J. J. Kai, F. R. Chen, and J. J. Lin, Nanotechnology **20**, 105203 (2009).
[26] A. Bid, A. Bora, and A. K. Raychaudhuri, Phys. Rev. B **74**, 035426 (2006).
[27] I. Hamberg, C. G. Granqvist, K. F. Berggren, B. E. Sernelius, and L. Engstrom, Phys. Rev. B **30**, 3240 (1984).
[28] Z. Q. Li and J. J. Lin, J. Appl. Phys. **96**, 5918 (2004).
[29] P. A. Lee and T. V. Ramakrishnan, Rev. Mod. Phys. **57**, 287 (1985).
[30] W. Niu, M. Gao, X. Wang, F. Song, J. Du, X. Wang, and Y. Xu, Sci. Rep. **6**, 26081 (2016).
[31] Y. Xu, J. Zhang, G. Cao, C. Jing, and S. Cao, Phys. Rev. B **73**, 224410 (2006).
[32] Y. Jin, X. L. Qian, B. Lu, S. X. Cao, and J. C. Zhang, RSC Adv. **5**, 2354 (2015).
[33] G. A. Wigger, E. Felder, S. Weyeneth, H. R. Ott, and Z. Fisk, Europhys. Lett. **68**, 685 (2004).
[34] A. A. Zvyagin and P. Schlottmann, Phys. Rev. B **54**, 15191 (1996).
[35] M. Hanl, A. Weichselbaum, T. A. Costi, F. Mallet, L. Saminadayar, C. Bauerle, and J. Von Delft, Phys. Rev. B **88**, 075146 (2013).
[36] T. A. Costi, L. Bergqvist, A. Weichselbaum, J. Von Delft, T. Micklitz, A. Rosch, P. Mavropoulos, P. H. Dederichs, F. Mallet, L. Saminadayar, and C. Bauerle, Phys. Rev. Lett. **102**, 056802 (2009).
[37] F. Mallet, J. Ericsson, D. Mailly, S. Unlubayir, D. Reuter, A. Melnikov, A. D. Wieck, T. Micklitz, A. Rosch, T. A. Costi, L. Saminadayar, and C. Bauerle, Phys. Rev. Lett. **97**, 226804 (2006).
[38] T. R. Mcguire and R. I. Potter, IEEE Trans. Magn. **11**, 1018 (1975).
[39] A. Kawabata, Solid State Commun. **34**, 431 (1980).
[40] G. Bergmann and F. Ye, Phys. Rev. Lett. **67**, 735 (1991).
[41] G. M. Alzoubi and N. O. Birge, Phys. Rev. Lett. **97**, 226803 (2006).

[42] N. W. Preyer, M. A. Kastner, C. Y. Chen, R. J. Birgeneau, and Y. Hidaka, Phys. Rev. B **44**, 407 (1991).
[43] K. Han, N. Palina, S. W. Zeng, Z. Huang, C. J. Li, W. X. Zhou, D.-Y. Wan, L. C. Zhang, X. Chi, R. Guo, J. S. Chen, T. Venkatesan, A. Rusydi, and Ariando, Sci. Rep. **6**, 25455 (2016).
[44] T. A. Costi, Phys. Rev. Lett. **85**, 1504 (2000).
[45] D. C. Langreth, Phys. Rev. **150**, 516 (1966).
[46] J. M. D. Coey, M. Venkatesan, and C. B. Fitzgerald, Nat. Mater. **4**, 173 (2005).
[47] F. A. Kröger and H. J. Vink, Solid State Phys. **3**, 307 (1956).
[48] G. B. González, T. O. Mason, J. P. Quintana, O Warschkow, D. E. Ellis, J.-H. Hwang, J. P. Hodges, and J. D. Jorgensen, J. Appl. Phys. **96**, 3912 (2004).
[49] K. S. Park, Y. J. Choi, J. G. Kang, Y. M. Sung, and J. G. Park, Nanotechnology **22**, 285712 (2011).